The influence of ligand charge and length on the assembly of *Brome mosaic virus* derived virus-like particles with magnetic core

Adam A. Mieloch,[1,2,a] Monika Kręcisz,[1,2,a] Jakub D. Rybka,[1,2,b] Aleksander Strugała,[1,3] Michał Krupiński,[4] Anna Urbanowicz,[3,5] Maciej Kozak,[6] Bohdan Skalski,[1] Marek Figlerowicz,[3,7,8] and Michael Giersig[1,2]

[1]*Faculty of Chemistry, Adam Mickiewicz University, 61-614 Poznan, Poland*
[2]*Centre for Advanced Technologies, Adam Mickiewicz University, 61-614 Poznan, Poland*
[3]*Institute of Bioorganic Chemistry, Polish Academy of Sciences, 61-704 Poznan, Poland*
[4]*The Henryk Niewodniczański Institute of Nuclear Physics, Polish Academy of Sciences, 31-342 Krakow, Poland*
[5]*Institute of Chemical Technology and Engineering, Poznan University of Technology, 60-965 Poznan, Poland*
[6]*Faculty of Physics, Adam Mickiewicz University, 61-614 Poznan, Poland*
[7]*Institute of Computing Science, Poznan University of Technology, 60-965 Poznań, Poland*
[8]*European Centre for Bioinformatics and Genomics, Poznań 60-965, Poland*

(Received 30 October 2017; accepted 25 February 2018; published online 5 March 2018)

Virus-like particles (VLPs) have sparked a great interest in the field of nanobiotechnology and nanomedicine. The introduction of superparamagnetic nanoparticles (SPIONs) as a core, provides potential use of VLPs in the hyperthermia therapy, MRI contrast agents and magnetically-powered delivery agents. Magnetite NPs also provide a significant improvement in terms of VLPs stability. Moreover employing viral structural proteins as self-assembling units has opened a new paths for targeted therapy, drug delivery systems, vaccines design, and many more. In many cases, the self-assembly of a virus strongly depends on electrostatic interactions between positively charged groups of the capsid proteins and negatively charged nucleic acid. This phenomenon imposes the negative net charge as a key requirement for the core nanoparticle. In our experiments, Brome mosaic virus (BMV) capsid proteins isolated from infected plants *Hordeum vulgare* were used. Superparamagnetic iron oxide nanoparticles (Fe_3O_4) with 15 nm in diameter were synthesized by thermal decomposition and functionalized with COOH-PEG-PL polymer or dihexadecylphosphate (DHP) in order to provide water solubility and negative charge required for the assembly. Nanoparticles were characterized by Transmission Electron Microscopy (TEM), Dynamic Light Scattering (DLS), Zeta Potential, Fourier Transformed Infrared Spectroscopy (FTIR) and Superconducting Quantum Interference Device (SQUID) magnetometry. TEM and DLS study were conducted to verify VLPs creation. This study demonstrates that the increase of negative surface charge is not a sufficient factor determining successful assembly. Additional steric interactions provided by longer ligands are crucial for the assembly of BMV SPION VLPs and may enhance the colloidal stability.
https://doi.org/10.1063/1.5011138

[a]equal contribution

[b]Corresponding Author: Dipl.-Ing. Dr.nat.techn. Jakub Rybka jrybka@amu.edu.pl, Centre for Advanced Technologies, Adam Mickiewicz University, ul. Umultowska 89C, 61-614 Poznan, Poland tel: +48 61 829 1875

INTRODUCTION

The definition of virus-like particles (VLPs) includes a plethora of biological structures related to viruses in terms of morphology, structure and self-assembly. In most cases, the term describes entities of viral origin subjected to structural or functional alterations e.g. capsids deprived of nucleic acid or genetically-modified capsid subunits. The most prominent characteristic of VLPs is their relative ease of creation through self-assembly of viral proteins. Due to a very broad spectrum of potential applications VLPs have been extensively studied for over three decades.[1,2] Combined effort of many research groups proved their exceptional utility as vaccines, gene-carrying nanocontainers, MRI contrast agents, drug-delivery vectors etc.[3–6]

Brome mosaic virus (BMV) is an icosahedral plant virus containing 4 ssRNA strands, incorporated within three separate particles. RNA1 and RNA2 are packaged separately, while RNA3 and RNA4 are co-packaged. The capsid forms a T=3 lattice and consists of 180 identical proteins. Subsequently, they form dimers and then, pentameric or hexameric subunits. Native form of the virus has the outer diameter of approximately 28 nm and the inner diameter of 18 nm. The mechanism of self-assembly is mainly driven by electrostatic interactions between positively charged arginine-rich motifs (ARMs) of the coat protein and negatively charged phosphate groups of the RNA.[7,8] The BMV capsid remains stable in buffers with pH below 5.0 and moderate ionic strength. The increase in pH above 7.5 and ionic strength higher than 0.5 M promotes capsid dissociation and allows for viral RNA precipitation. Decrease of the pH and ionic strength back to previous values initiates reassembly of the capsid.[9] This approach has been utilized in creation of BMV VLPs containing various cores e.g. gold nanoparticles, quantum dots, magnetite nanoparticles.[9–11]

BMV can be obtained through infection of various hosts. Importantly, the physicochemical differences between virions produced in barley, wheat and *Nicotiana benthamiana* are not trivial. The study done by Ni *et al.,* revealed host-specific variations in electrostatic charges, isoelectric profiles and capsid-RNA interactions of the virions. These parameters were shown to affect thermal stability of the capsid.[12] Obtained data indicates that the host effects plays an important role in the self-assembly of the VLPs and has to be taken into consideration while drawing conclusions regarding BMV VLPs assembly mechanisms.

Superparamagnetic iron oxide nanoparticles (SPIONs) have a set of unique magnetic and physicochemical characteristics qualifying them as a promising tool in many biomedical applications. High-yield production methods, low-toxicity and tunable surface and magnetic properties render them exceptionally useful in many applications e.g. contrast agent in MRI, magnetically driven carrier in targeted drug delivery or in magnetic hyperthermia for cancer treatment, etc.[13–17] Theoretical studies done by Kusters *et al.* indicates that the core size polydispersity, as low as 1%, strongly affects the assembly efficiency.[18] Therefore, high monodispersity of SPIONs is an essential prerequisite.

In our study, 15 nm in diameter SPIONs were obtained *via* thermal decomposition of iron (III) acetylacetonate in organic solvent. This method provides high quality and quantity of the SPIONs.[19] Obtained nanoparticles contain oleic acid residues on the surface. Further functionalization was required to obtain water solubility and negative charge on the surface of the SPIONs. Two compounds were chosen for the experiment: distearoyl-sn-glycero-3-phosphoethanolamine-N-[carboxy-(PEG)2000] (HOOC-PEG-PL), used in similar experiments by Dragnea *et al.*, and dihexadecylphosphate (DHP).[10] We estimated, that 15 nm particles after functionalization will have ~ 18 nm in diameter, which is commensurate with inner cavity of BMV T=3 capsid. Both compounds share similar mechanism of functionalization through hydrophobic interactions between oleic acid residues on the surface of the SPIONs and twin alkyl chains. Our study investigates how different values of negative surface charge and steric effects influence the process of BMV self-assembly on functionalized SPIONs.

RESULTS AND DISCUSSION

Superparamagnetic iron oxide nanoparticles (SPIONs) synthesis

SPIONs were synthesized *via* modified route of iron (III) acetylacetonate thermal decomposition in 1-octadecene with oleic acid as surfactant (NP OA).[20] Obtained nanoparticles were analyzed with

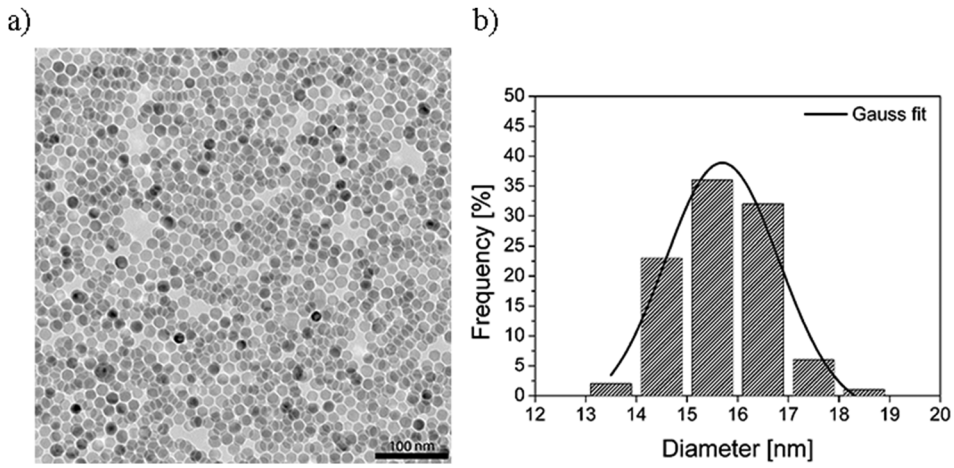

FIG. 1. **a)** SPIONs synthetized via thermal decomposition of $Fe(acac)_3$ suspended in chloroform visualized in TEM. **b)** SPIONs size distribution histogram.

TEM (Figure 1a). Data shows that 15.70 ± 0.95 nm in diameter nanoparticles were spherical and monodispersed (Figure 1b).

Magnetic behavior of SPIONs

Magnetic properties of the obtained nanoparticles were assessed with SQUID magnetometry. Magnetic coercivity (H_c) of the 15.7 nm at 300K is close to 0 Oe, which means that there is no energy dissipated during repeated reversing of magnetization – defining the material as superparamagnetic (Figure 2b). Magnetic saturation at this temperature (M_s) equals 39.6 emu/g (Figure 2b). Blocking temperature obtained from zero field cooling and field cooling (ZFC-FC) measurement is 139 K (Figure 2a). Below blocking temperature at 5 K, H_c = 700 Oe and M_s = 42.9 emu/g (Figure 2c).

SPIONs functionalization

As synthesized, SPIONs surface is covered in alkyl chains of oleic acid rendering them hydrophobic. Two compounds were used for functionalization: COOH-PEG-PL copolymer and dihexadecylphosphate (DHP) (Figure 3). Both compounds functionalize the surface of SPIONs through hydrophobic interactions between oleic acid residues and alkyl chains, creating micelles. COOH-PEG-PL has been successfully used as a coating agent in previous studies regarding BMV assembly with magnetic cores.[10] The main drawbacks of this compound is its cost and low availability, which drastically decreases commercial potential. Our goal was to find an alternative compound providing negative surface charge density sufficient for self-assembly.[21] DHP is a anionic surfactant molecule with two alkyl chains and negatively charged phosphate group, which has been widely utilized in the field of electrochemical sensing and biosensing.[22] Due to explicit differences in structure, we

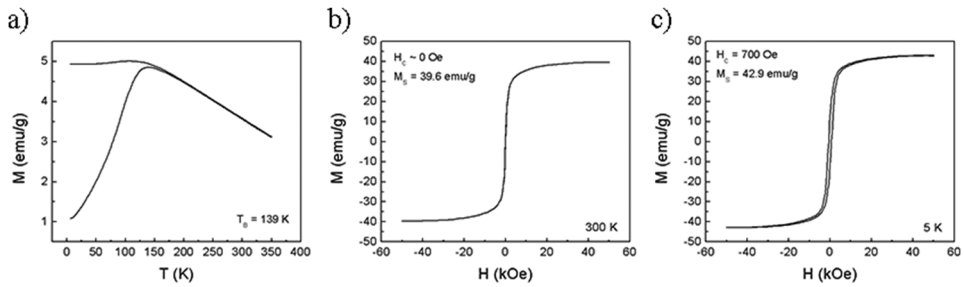

FIG. 2. SQUID magnetometry of the SPIONs. **a)** ZFC-FC, blocking temperature **b)** Magnetic coercivity (H_c) and magnetic saturation (M_s) at 300K. **c)** H_c and M_s at 5K.

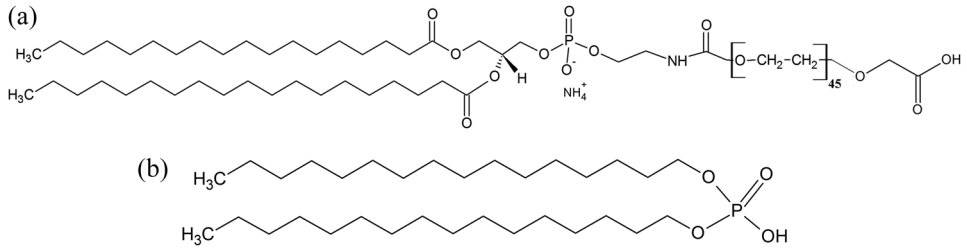

FIG. 3. Molecular structure of ligands used to functionalize SPIONs. a) COOH-PEG-PL. b) DHP.

decided to investigate whether the presence of long polymer chain is as a prerequisite for BMV VLPs creation. Zeta potential analysis revealed the difference in values between functionalized SPIONs: DHP = -56.6 ± 0.7 mV (further referred as NP DHP), COOH-PEG-PL = -31 ± 0.4 mV (further referred as NP PEG) (Figure 4). We assumed that higher value of total negative charge could compensate for possible low ligand density and still provide sufficient surface charge density required for self-assembly. Hydrodynamic diameter of the functionalized SPIONs was assessed using Dynamic Light Scattering (DLS) measurement (Figure 5a). NP PEG were 57 ± 15 nm in diameter. NP DHP had slightly smaller diameter of 52 ± 12 nm. Broad distributions and significant standard deviations of size diameters for both DLS measurements can be related with particles size distribution revealed with TEM analysis.

Fourier Transformed Infrared Spectroscopy (FTIR) analyses showed that all spectra for nanoparticles contain peaks around 574 cm^{-1} and 623 cm^{-1} originating from stretching vibrations of Fe-O, which confirm existence of iron oxide nanoparticles (Figure 6).[23,24] Peaks around 1400 cm^{-1} and 1630 cm^{-1} on the NP OA spectrum can be attributed to the symmetric and assymetric stretching of carboxylate (COO-), which refers to the binding between iron oxide and oleic acid.[25,26] Broad peaks in the region between 3200 – 3600 cm^{-1} visible in almost all spectra, can be assigned to the vibrations of the hydroxyl group (OH^-). Strong absorption bands around 3400 cm^{-1} can also originate from bonds of nanoparticles‘ surface.[23,24] Stretchings of double bonded C=O group are also visible around 1700 cm^{-1} on spectra for nanoparticles and pure PEG. All spectra contain sharp peaks in the range of 2800 – 3000 cm^{-1} assigned to the vibrations of the C-H group.[23] We assumed that functionalization process was successful for either PEG and DHP polymer due to the shifts of asymmetric and symmetric CH_2 vibrations and presence of characteristic peaks. On the spectrum of nanoparticles with oleic acid we established high values of wavenumbers for those vibrations. It can be correlated with conformation of the alkyl chains – *trans* and *gauche* isomers. Shift toward lower wavenumbers for functionalised particles indicates that more chains are in *trans* conformation and particles are in more ordered state.[27,28] Characteristic sharp peak around 1111 cm^{-1} visible on spectra for pure

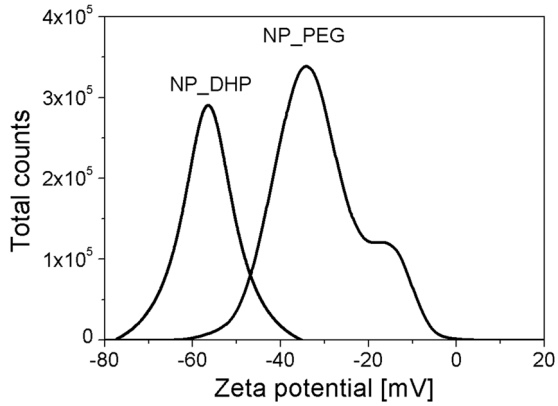

FIG. 4. Zeta potential measurement of SPIONs functionalized with DHP (NP_DHP) and COOH-PEG-PL (NP_PEG).

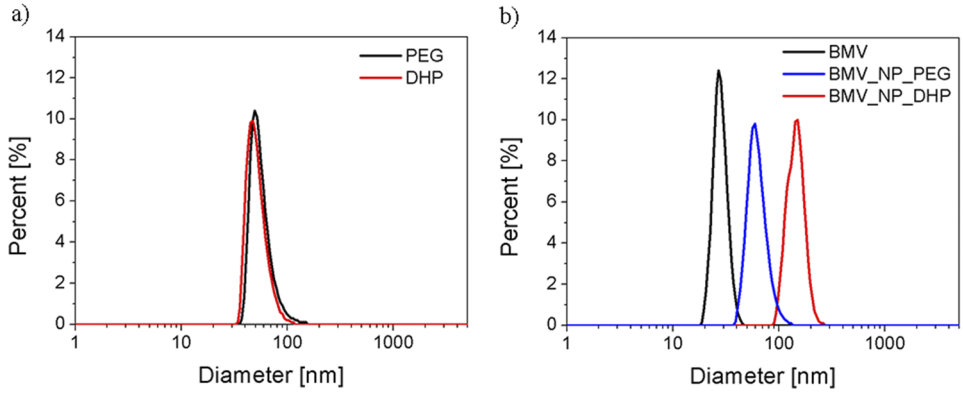

FIG. 5. Number-based particle size distributions of **a)** SPIONs functionalized with DHP and COOH-PEG-PL (PEG) **b)** VLPs assembled with magnetic cores and native BMV.

PEG and nanoparticles functionalised with this polymer correspond to the stretching vibrations of C-O-C group from repeated units of the polyethylene glycol backbone.[28] On the spectra for pure polymers and functionalised particles we can also see peaks connected with other CH_2 group vibrations - wagging (1350 cm^{-1}), twisting (1250 cm^{-1}) of CH_2 and scissoring bands in the range of 1430-1490. Peaks from asymmetric and symmetric stretching of PO_2^- group can also be found on those spectra.[28]

VLPs assembly

The assembly of BMV NP PEG was performed according to previously published protocol.[10]

The native structure of synthesized virus is shown in Fig. 7a, in this cryo-microscopic image the monodisperse without defects structure is clearly visible. In followed TEM images the core-shell structures (magnetic core and protein shell) was the superparamagnetic particles was in ca 90% of viruses detected (see Figure 7b). Calculated size of the VLPs was 26.4 ± 2.1 nm which is similar to diameter of the native BMV ~28 nm. This indicates T=3 capsid symmetry as shown in other studies.[9] Calculated thickness of the shell was 5.20 ± 0.03 nm, which also corresponds to the native form of the BMV.[8] This method provided well separated VLPs containing only one core particle

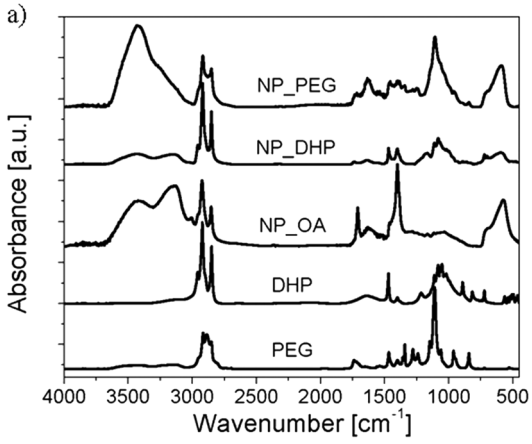

b)

	NP_PEG	NP_DHP	NP_OA	DHP	PEG
ν_s CH_2 vibrations [cm^{-1}]	2850.7	2851.6	2853.2	2850.9	2850.5
ν_{as} CH_2 vibrations [cm^{-1}]	2918.0	2919.7	2924.5	2923.0	2917.5

FIG. 6. FTIR spectra of functionalization intermediates and products **a)** with wavenumber characteristic **b)** of their symmetric (ν_s) and asymmetric (νa_s) stretching CH_2 vibrations.

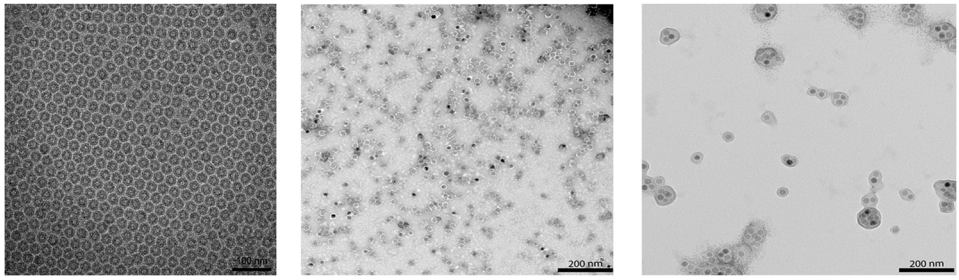

FIG. 7. TEM images of the assembled VLPs. **a)** cryo TEM images of natives BMV virus **b)** BMV VLPs with COOH-PEG-PL functionalized SPIONs as core **c)** BMV VLPs with DHP functionalized SPIONs as core.

in majority. In case of BMV NP DHP assembly, applying the same protocol did not result in VLPs creation. Mixing NP DHP with BMV dimers in the assembly buffer, resulted in precipitation and no VLPs were created. According to our experience drawn from HBcAg assembly studies, NP DHP proved stable in phosphate/citrate buffer. Abiding the rationale behind BMV self-assembly, modified assembly buffer has been introduced. This approach has been successful and resulted in BMV DHP VLPs formation (Figure 7b). Obtained VLPs were 25.5 ± 2.7 nm in diameter. The thickness of the shell was 5.53 ± 0.97 nm. This indicates that despite different coatings, the result of the assembly is similar. However, in case of BMV DHP VLPs, many multicore aggregates were also formed. One of possible explanations for this result is a gradual neutralization of the surface charge by BMV capsid proteins, leading to deprivation of electrostatic repulsive forces. Gradually decreasing stability of NP DHP could significantly facilitate formation of multicore and aggregated VLPs. In case of NP PEG, colloid stability is achieved through both steric and electrostatic interactions. Therefore, neutralization of the surface charge does not attenuate overall stability sufficiently to disturb the assembly, leaving the steric component intact. Our studies also showed longer storage stability of BMV NP PEG, which can be attributed to two characteristics: higher amount of well dispersed single core VLPs and some portion of PEG tails protruding out of VLP through protein shell, adding to its stability. Comparative study by Malyutin *et al.* revealed the behavior of poly(ethylene glycol) tails in BMV and hepatitis B virus (HBV) VLPs, indicating that in case of BMV VLPs majority of tails remain entrapped between the core and the protein layer. Weather the remaining fraction of protruding PEG tails contributes significantly to the increased stability, remains to be elucidated. Dynamic Light Scattering measurements revealed hydrodynamic diameters of VLPs (Figure 5b). Number distributions and hydrodynamic diameters of native BMV established at 28.1 ± 4.4 nm. BMV NP PEG diameter was established at 63 ± 13 nm and it is larger than diameter for both pure nanoparticles with PEG polymer and native BMV, which was also measured by DLS and appointed at 28.1 ± 4.4 nm. BMV NP DHP diameter shifted toward higher values of 145 ± 27 nm. Such high value of the hydrodynamic diameter in comparison with diameters of the native BMV and nanoparticles with DHP polymer, can be related with possibility of clusters or aggregates formation during the assembly process.

CONCLUSIONS

Our study demonstrates how electrostatic and steric properties of the functionalized SPIONs govern the process of the BMV VLPs assembly. Usage of PEG tail containing COOH-PEG-PL compound as a functionalizing agent resulted in well dispersed single core VLPs. DHP functionalized SPIONs required major modifications in the assembly buffer composition. This resulted in BMV VLPs creation, however obtained particles formed many clusters and fewer single core VLPs could be found. Obtained results indicate that nanoparticles stabilized solely through electrostatic interactions may require different approach in core containing VLPs creation. The lack of steric stabilization poses a disadvantage in terms of VLPs assembly, morphology and storage stability.

MATERIALS AND METHODS

Materials

Oleic acid (technical grade 90%), Iron (III) acetylacetonate (97%), Sodium chloride (99%), Dihexadecyl phosphate, 1-Octadecene (90%), 2-Butanol (95.5%), Trizma® base (99.9%), Calcium chloride (97%), Magnesium chloride (98%), Magnesium acetate tetrahydrate (99%), Sodium acetate (99%), Glycine (99%), Glycerol (99%), Citric acid (99.5%), Sodium phosphate dibasic (99%) Sigma-Aldrich (Poznan, Poland). Toluene (99.5%), n-Hexane (99%), Chloroform (98.5%), Hydrochloric acid (30-35%), Avantor (Gliwice, Poland). Boric acid (99%), ICN biomedicals (USA). PEG 8000 (reagent grade) BioShop (Canada). 1,2-Distearoyl-sn-glycero-3-phosphoethanolamine-N-[carboxy-(polyethylene glycol)2000] (ammonium salt) (COOH-PEG- PL, 2000 Da PEG (99%) Avanti (USA). Snakeskin® Dialysis Tubing 10K MWCO, Thermo Fisher Scientific (USA). All chemicals were used as received. Water was purified by Hydrolab HLP5 instrument (0.09 μS/cm).

Methods

Synthesis of iron oxide nanoparticles

Spherical iron oxide nanoparticles were synthesized by thermal decomposition of iron (III) acetylacetonate $Fe(acac)_3$. Briefly, 6 mmol of $Fe(acac)_3$ and 12 mmol of oleic acid were dissolved in 40 ml of 1-octadecene. The reaction was performed with continuous stirring and nitrogen flow. Temperature of the solution was increased to 220 °C and maintained for 1 hour. Then, the temperature was increased further to 320 °C and maintained for 1 hour. After synthesis, 3:1 v/v mixture of 2-butanol and toluene was added and the solution was placed on neodymium magnet to precipitate. The precipitate was washed thrice with the same mixture. Obtained nanoparticles were suspended in chloroform. Nanoparticles concentration was estimated by weighing dried sample.

Functionalization of iron oxide nanoparticles with COOH-PEG-PL (NP PEG)

Functionalization was performed according to method published elsewhere,[10] with minor modifications. Briefly, 2.5 mg COOH-PEG-PL was added to chloroform solution containing 3 mg of as synthesized nanoparticles coated with oleic acid. The sample was shortly sonicated and left open for chloroform evaporation. Obtained waxy solid was heated for 1 min in 80 °C water bath. Then, 1 ml of water was added and the sample was vortexed to enhance micelles formation. Subsequently, the sample was washed thrice with chloroform to remove unbound COOH-PEG-PL. In order to remove chloroform residuals, the sample was diluted with water to total volume of 10 ml and centrifuged for 20 min at 12 000 x g, RT. Supernatant was discarded and the precipitate redispersed in 1 ml of water. Nanoparticles concentration was estimated by weighing dried sample.

Functionalization of iron oxide nanoparticles with dihexadecyl phosphate (DHP) (NP DHP)

The protocol describing in-depth preparation and characterization of DHP coated NP is in preparation and will be published at later date. Briefly, 6 mg of DHP was dissolved in 20 ml of hexane. Dissolution was heat-assisted at 75°C. Then, chloroform solution containing 6.3 mg of as synthesized nanoparticles coated with oleic acid was added and kept at 75°C for 10 min to allow for alkyl chains relaxation. The mixture was shortly sonicated and 80 ml of water was added. Subsequently, obtained two phase solution was briefly vortexed and sonicated until the water phase became turbid. In the next step, the solution was placed in sonicating bath for 3-4 h without temperature control. The reaction was continued until the mixture became homogenous and no signs of phase separation occurred for at least 1 min after mixing. After functionalization, the solution was left undisturbed overnight to allow for phase separation. Bottom phase was collected, filtered through 0.45 μm pores and centrifuged for 20 min at 10 000 x g, 4°C. Centrifugation was repeated until no precipitate was found. Collected precipitate was redispersed in water and filtered through 0.22 μm pores. Final concentration was measured by weighing dried sample.

BMV propagation, extraction and purification

BMV virions were multiplied in *Hordeum vulgare* plants. Briefly, after inoculation and incubation period, frozen leaves were homogenized in liquid nitrogen and macerated in a virus extraction

buffer (0.5 M NaOAc, 0.3 M H_3BO_3, 0.01 M $MgCl_2$, pH 4.5). The mixture was subjected to chloroform extraction and the virus was precipitated from the aqueous phase with PEG 8000. Virions were purified by ion exchange chromatography and concentrated using Amicon Ultra Filter 100 kDa (Merck Millipore) to 2 ml volume. Obtained sample was additionally purified by size-exclusion chromatography (SEC) and once more concentrated by previously mentioned method.

VLPs assembly protocol (BMV PEG VLPs, BMV DHP VLPs)

Virus like particles were prepared according to modified protocol for encapsulation of nanoparticles in BMV coat proteins.[29] BMV virions were dissociated in disassembly buffer: 1 M $CaCl_2$, 0.005 M Trizma®Base, pH 7.4, purified *via* centrifugation (13 000 g, 20 min, 4°C) and dialysed against desalting buffer (0.01 M Trizma®Base, pH 7.4). Obtained BMV dimers were dialysed against storage in buffer with high ionic strength: 1 M KCl, 0.005 M MgCl2, 0.01 M Trizma®Base, pH 7.4. NP PEG and BMV coat proteins (present as dimers) were mixed at 1:3 ratio (NP:BMV) and dialysed against assembly buffer: 0.01 M KCl, 0.05 M NaCl, 0.005 M MgCl2, 0.05 M Trizma®Base, pH 7.4. After encapsulation VLPs were dialysed against low ionic strength storage buffer: 0.05 M NaOAc, 0.008 M $Mg(OAc)_2$, pH 4.6. Encapsulation of NP_DHP was performed in the same ratio (1:3) and dialysed against modified assembly buffer (0.15 M NaCl, 0.01 M $CaCl_2$, 1% w/v Glycine, 10% v/v Glycerol, 0.03 M Citric acid, 0.05 M Na_2HPO_4, pH 4.5 and stored in the same buffer. All dialyses were performed with Snakeskin® Dialysis Tubing 10K MWCO.

Characterization methods

Transmission electron microscopy (TEM) images were acquired with Hitachi TEM HT7700 microscope. Grids were made of copper coated with carbon film, mesh 300. Samples of functionalized nanoparticles were prepared by placing 15 μl drop on the grid and draining the excess solution with blotting paper. Samples of assembled VLPs were prepared similarly. VLPs samples were additionally negatively stained with 5 μl of 2% uranyl acetate. Particle size analysis was performed with ImageJ software. At least 50 particles were analyzed.

Hysteresis loops at 5K and 300 K and ZFC-FC plots were obtained with SQUID MPMS XL Quantum Design system. The zero field-cooled (ZFC) and field-cooled (FC) magnetization curves were obtained using a standard protocol. After demagnetization at 300 K the system was cooled to 5 K without a magnetic field. Then, an external magnetic field of 100 Oe was applied, and the ZFC curve was recorded during heating to 300 K. The FC curve was measured during cooling from 300 K down to 5 K in the same external magnetic field.

Zeta potential measurement was performed on Particulate Systems NanoPlus instrument in standard zeta cell with dome electrode. Measurements were repeated in triplicate.

DLS measurement was performed on Malvern Zetasizer μV instrument in quartz cuvette (QS Hellma, Type 105.231 – 1 cm path-length). Before measurement samples were briefly sonicated, diluted to optimal concentration and filtered with 0.2 μm syringe filter. Measurements were repeated in triplicate.

Fourier Transformed Infrared Spectroscopy (FTIR) was used to confirm nanoparticles functionalization. Samples were dried, mixed with KBr and pressed into pellets before measurement. Spectra were obtained on TENSOR 27 (Bruker Optics) in the range of4000 - 400 cm^{-1} with a resolution of 4 cm^{-1}, and accumulation of 256 scans.

BMV concentrations were determined via UV-Vis absorption (NanoDrop 2000 spectrophotometer) and Lambert-Beer's law. Proteins concentration were established with absorbance at 280 nm.

ACKNOWLEDGMENTS

This work was supported by UMO-2012/06/A/ST4/00373 grant from National Science Centre (Poland).

The authors declare no financial or commercial conflicts of interest.

[1] C. Liu, S.-H. Chung, Q. Jin, A. Sutton, F. Yan, A. Hoffmann, B. K. Kay, S. D. Bader, L. Makowski, and L. Chen, "Magnetic viruses via nano-capsid templates," J. Magn. Magn. Mater. **302**, 47–51 (2006).
[2] J. Yun, A. M. Sonabend, I. V. Ulasov, D.-H. Kim, E. A. Rozhkova, V. Novosad, S. Dashnaw, T. Brown, P. Canoll, J. N. Bruce *et al.*, "A novel adenoviral vector labeled with superparamagnetic iron oxide nanoparticles for real-time tracking of viral delivery," J. Clin. Neurosci. **19**, 875–880 (2012).
[3] D. Gao, X. Lin, Z. Zhang, W. Li, D. Men, X. Zhang, and Z. Cui, Intracellular Cargo Delivery by Virus Capsid State Key Laboratory of Virology, Wuhan Institute of Virology Chinese Academy of Nanomedicine Nanotechnology, Biol. Med. (2015).
[4] K. M. Frietze, D. S. Peabody, and B. Chackerian, "Engineering virus-like particles as vaccine platforms," Curr. Opin. Virol. **18**, 44–49 (2016).
[5] J. L. Sagaseta, E. Malito, R. Rappuoli, and M. J. Bottomley, "Self-assembling protein nanoparticles in the design of vaccines," Comput. Struct. Biotechnol. J. **14**, 58–68 (2015).
[6] A. G. Malyutin, R. Easterday, Y. Lozovyy, A. Spilotros, H. Cheng, O. R. Sanchez-Felix, B. D. Stein, D. G. Morgan, D. I. Svergun, B. Dragnea *et al.*, "Viruslike nanoparticles with maghemite cores allow for enhanced MRI contrast agents," Chem. Mater. **27**, 327–335 (2015).
[7] C. C. Kao and K. Sivakumaran, "Brome mosaic virus, good for an RNA virologist's basic needs," Mol. Plant Pathol. **1**, 91–97 (2000).
[8] A. L. N. Rao, "Molecular studies on bromovirus capsid protein," Virology **232**, 385–395 (1997).
[9] J. Sun, C. DuFort, M.-C. Daniel, A. Murali, C. Chen, K. Gopinath, B. Stein, M. De, V. M. Rotello, A. Holzenburg *et al.*, "Core-controlled polymorphism in virus-like particles," Proc. Natl. Acad. Sci. **104**, 1354–1359 (2007).
[10] X. Huang, L. M. Bronstein, J. Retrum, C. Dufort, I. Tsvetkova, S. Aniagyei, B. Stein, G. Stucky, B. McKenna, N. Remmes *et al.*, "Self-assembled virus-like particles with magnetic cores," Nano Lett. **7**, 2407–2416 (2007).
[11] S. K. Dixit, N. L. Goicochea, M. C. Daniel, A. Murali, L. Bronstein, M. De, B. Stein, V. M. Rotello, C. C. Kao, and B. Dragnea, "Quantum dot encapsulation in viral capsids," Nano Lett. **6**, 1993–1999 (2006).
[12] P. Ni, R. C. Vaughan, B. Tragesser, H. Hoover, and C. C. Kao, "The plant host can affect the encapsidation of brome mosaic virus (BMV) RNA: BMV virions are surprisingly heterogeneous," J. Mol. Biol. **426**, 1061–1076 (2014).
[13] A. Petri-fink, M. Chastellain, L. Juillerat-jeanneret, A. Ferrari, and H. Hofmann, "Development of functionalized superparamagnetic iron oxide nanoparticles for interaction with human cancer cells **26**, 2685–2694 (2005).
[14] W. Wu, Z. Wu, T. Yu, C. Jiang, and W.-S. Kim, "Recent progress on magnetic iron oxide nanoparticles: Synthesis, surface functional strategies and biomedical applications," Sci. Technol. Adv. Mater. **16**, 23501 (2015).
[15] E. Amstad, M. Textor, and E. Reimhult, "Stabilization and functionalization of iron oxide nanoparticles for biomedical applications," Nanoscale **3**, 2819 (2011).
[16] S. Klein, A. Sommer, L. V. R. Distel, W. Neuhuber, and C. Kryschi, "Superparamagnetic iron oxide nanoparticles as radiosensitizer via enhanced reactive oxygen species formation," Biochem. Biophys. Res. Commun. **425**, 393–397 (2012).
[17] A. Silva, É. Silva-Freitas, and J. Carvalho, "Magnetic particles in biotechnology: From drug targeting to tissue engineering," Adv. Appl. Biotechnol. 237–256 (2012).
[18] R. Kusters, H.-K. Lin, R. Zandi, I. Tsvetkova, B. Dragnea, and P. van der Schoot, "Role of charge regulation and size polydispersity in nanoparticle encapsulation by viral coat proteins," J. Phys. Chem. B **119**, 1869–1880 (2015).
[19] M. Giersig and M. Hilgendorff, "Magnetic nanoparticle superstructures," Eur. J. Inorg. Chem. 3571–3583 (2005).
[20] S. Sun, H. Zeng, D. B. Robinson, S. Raoux, P. M. Rice, S. X. Wang, and G. Li, "Monodisperse MFe2O4 (M = Fe, Co, Mn) nanoparticles," J. Am. Chem. Soc. **126**, 273–279 (2004).
[21] M. C. Daniel, I. B. Tsvetkova, Z. T. Quinkert, A. Murali, M. De, V. M. Rotello, C. C. Kao, and B. Dragnea, "Role of surface charge density in nanoparticle-templated assembly of bromovirus protein cages," ACS Nano **4**, 3853–3860 (2010).
[22] B. C. Janegitz, M. Baccarin, P. A. Raymundo-Pereira, F. A. Dos Santos, G. G. Oliveira, S. A. S. Machado, M. R. V. Lanza, O. Fatibello-Filho, and V. Zucolotto, "The use of dihexadecylphosphate in sensing and biosensing," Sensors and Actuators, B: Chemical **220**, 805–813 (2015).
[23] J. Sangeetha, S. Thomas, J. Arutchelvi, M. Doble, and J. Philip, "Functionalization of iron oxide nanoparticles with biosurfactants and biocompatibility studies," J. Biomed. Nanotechnol. **9**, 751–764 (2013).
[24] I. Karimzadeh, M. Aghazadeh, M. R. Ganjali, T. Doroudi, and P. H. Kolivand, "Preparation and characterization of iron oxide (Fe 3 O 4) nanoparticles coated with polyvinylpyrrolidone/polyethylenimine through a facile one-pot deposition route," J. Magn. Magn. Mater. **433**, 148–154 (2017).
[25] A. G. Roca, M. P. Morales, K. O'Grady, and C. J. Serna, "Structural and magnetic properties of uniform magnetite nanoparticles prepared by high temperature decomposition of organic precursors," Nanotechnology **17**, 2783–2788 (2006).
[26] L. Zhang, R. He, and H. C. Gu, "Oleic acid coating on the monodisperse magnetite nanoparticles," Appl. Surf. Sci. **253**, 2611–2617 (2006).
[27] F. G. Wu, J. J. Luo, and Z. W. Yu, "Infrared spectroscopy reveals the nonsynchronicity phenomenon in the glassy to fluid micellar transition of DSPE-PEG2000 aqueous dispersions," Langmuir **26**, 12777–12784 (2010).
[28] C. Yue-Jian, T. juan, X. Fei, Z. Jia-Bi, G. Ning, Z. Yi-Hua, D. Ye, and G. Liang, "Synthesis, self-assembly, and characterization of PEG-coated iron oxide nanoparticles as potential MRI contrast agent," Drug Dev. Ind. Pharm. **36**, 1235–1244 (2010).
[29] B. P. Orner, *Protein Cages* (2015), Vol. 1252.